Electron cyclotron current drive in low collisionality limit: on parallel momentum conservation

N. B. Marushchenko,[1,*] C. D. Beidler,[1] S. V. Kasilov,[2,3]
W. Kernbichler,[3] H. Maaßberg,[1] R. Prater,[4] and R. W. Harvey[5]

[1] *Max-Planck-Institut für Plasmaphysik, IPP-EURATOM Association, D-17491 Greifswald, Germany*
[2] *Institute of Plasma Physics, National Science Center "Kharkov Institute of Physics and Technology", Akademicheskaya 1, 61108 Kharkov, Ukraine*
[3] *Institut für Theoretische Physik - Computational Physics, Technische Universität Graz, Association EURATOM-ÖAW, Petergasse 16, A8010 Graz, Austria*
[4] *General Atomics, PO Box 85608, San Diego, CA 92186-5608, USA*
[5] *CompX, PO Box 2672, Del Mar, CA 92014, USA*

(Dated: March 2, 2011)

A comprehensive treatment of the models used in ray- and beam-tracing codes to calculate the electron cyclotron current drive (ECCD) by means of the adjoint technique, based on the adjoint properties of the collision and Vlasov operators appearing in the drift-kinetic equation, is presented. Particular attention is focused on carefully solving the adjoint drift-kinetic equation (generalized Spitzer problem) with parallel momentum conservation in the like-particle collisions. The formulation of the problem is valid for an arbitrary magnetic configuration. Only the limit of low collisionality is considered here, which is of relevance for high-temperature plasmas. It is shown that the accurate solution of the adjoint drift-kinetic equation with parallel momentum conservation significantly differs (apart from the supra-thermal electron portion) from that calculated in the high-speed-limit, which is most commonly used in the literature. For high-temperature plasmas with significant relativistic effects, the accuracy of the resulting numerical models is demonstrated by ray-tracing calculations and benchmark results are presented. It is found that the ECCD efficiency calculated for ITER with parallel momentum conservation significantly exceeds the predictions obtained with the high-speed-limit model.

I. INTRODUCTION

Starting from the proposals of Ohkawa [1] and Fisch-Boozer [2], electron cyclotron current drive (ECCD) has been developed into one of the primary tools for the non-inductive creation of current in plasmas. Having been intensively studied theoretically [3–8] and experimentally [8–11], ECCD is sufficiently well understood for practical applications in both tokamaks (control of the MHD activity) and stellarators (compensation of the bootstrap-current). The main numerical tools for calculation of ECCD combine the adjoint technique with ray tracing and a number of such solvers have been developed and successfully applied [5, 7]. Apart from this, the ECCD efficiency in tokamaks can be calculated directly by the bounce-averaged Fokker-Planck solver [12]. Despite qualitative agreement of theoretical predictions with experimental results, a number of discrepancies exists. For example, it was found [13] that the Fokker-Planck calculations agree much better with the experiment than the calculations by the adjoint technique in the widely used high-speed-limit approach. This result was interpreted as a consequence of neglecting parallel momentum conservation in the latter. Apart from this, it was also found [14] that in some scenarios the measured current drive can significantly exceed the value predicted by bounce-averaged Fokker-Planck calculations with trapped particles, being instead much closer to the value calculated without trapped particles. A leading candidate for explanation of these findings is the effect of finite collisionality for which the contribution barely trapped electrons becomes non-negligible. As a consequence, the validity and the range of applicability for theoretical models must be revised after undergoing careful analysis.

The adjoint technique proposed in Refs. 15, 16 is an advanced and convenient method for calculation of the current drive in plasmas. Moreover, only this technique is applicable for stellarators as the bounce-averaged Fokker-Planck model explicitly assumes axisymmetric configurations. Formally, the applicability of the adjoint technique is limited by the natural condition that the plasma response to the rf source in electron cyclotron resonance heating (ECRH) remains linear, i.e. when the density of the RF power, P_{RF}, is sufficiently low in comparison with the rate of collisional thermalization, $\kappa_{\mathrm{lin}} = P_{\mathrm{RF}}/n_e T_e \nu_e \simeq 2.86\times10^{-4} P_{\mathrm{RF}}\sqrt{T_e}/(n_{20}^2(1+Z_{\mathrm{eff}}))\cdot x_r^3 \ll 1$, but practically, the standard ECRH/ECCD scenarios (especially in large machines) easily satisfy this condition (here, P_{RF} in MW/m^3, T_e in keV, $n_{20} = n_e/10^{20}$, $\nu_e(v) = \nu_{ee}(v) + \nu_{ei}(v)$ is the electron collision frequency, and $x_r = v_{\mathrm{res}}/v_{\mathrm{th}}$ with $v_{\mathrm{th}} = \sqrt{2T_e/m}$ is the normalized resonance velocity which corresponds to the maximum contribution in the absorption). The central idea of the adjoint technique is exploiting the self-adjoint properties of the linearized collision operator to express the current through the (steady state) adjoint Green's function,

*Electronic address: nikolai.marushchenko@ipp.mpg.de

which is proportional to the linear plasma response in the presence of a parallel electric field that is formally identical to the solution of the Spitzer problem [17–21]. The effectiveness of this method was demonstrated first for calculation of the electron fraction of the current driven by a neutral beam in a homogeneous magnetic field [15], and was then repeated with toroidicity accounted for [22]. This technique was subsequently applied also to determine the current generated by different kinds of RF sources [5–7, 16, 23–27]. At present, the adjoint technique is commonly used for calculations of electron cyclotron current drive in different ray- and beam-tracing codes (see for example Ref. 28 and the references therein).

The key point of the adjoint technique is the choice of model for the corresponding response function, which is commonly referred to as the Green's function. Formally, in toroidal plasmas (not necessarily axisymmetric), the adjoint 4D drift kinetic equation (3D in tokamaks) must be solved while taking into account such factors as the geometry of the problem, the small but finite collisionality, conservation of parallel momentum, relativity, etc. Due to toroidicity, the problem can be reduced to an easily solvable level only for two opposite limits. In the highly collisional (classical) limit, where $\nu_e^* \gg 1$ (here, $\nu_e^* = \nu_e R/\iota v$ is the collisionality, R and ι are the major radius and the rotational transform, respectively), trapped particles do not play any role and the problem can be reduced to the classical Spitzer problem of calculation of the electric conductivity in un-magnetized plasmas. The value of current drive efficiency calculated with this approach [2, 3] usually corresponds to the upper theoretical limit. In the opposite, low collisionality (or collisionless) limit, where $\nu_e^* \ll 1$, the trapped particles do not contribute to the current drive, and produce a non-negligible drag on the passing particles. (In this limit, kinetic models with bounce-averaging are applicable.) This model, which is accepted as most relevant to ECCD calculations in toroidal plasmas [5–7, 23–27], usually tends to underestimate the current drive efficiency as it neglects all effects due to (barely) trapped electrons. For this model, the drag over the trapped electrons is assumed to be equal to its upper "geometrical" limit. The intermediate regime, where finite collisionality effects become significant, will not be considered here but will be treated in a future paper.

Historically, for calculation of ECCD, the linearized collision operator in the drift kinetic equation was simplified by using the high-speed-limit (*hsl*) approach [3, 5, 7], where only pitch-angle scattering and the drag were taken into account. This approach is questionable even for low temperature plasmas and surely not sufficient for high temperature plasmas. For plasmas with ITER-like parameters, the high-speed-limit can lead (depending on the scenario) to significant underestimation of the current drive efficiency for the main ECRH/ECCD scenarios [28, 29].

Another point which requires attention is the necessity to take relativistic effects into account. Contrary to transport theory, where these effects are of rather minor importance (at least, for modern fusion devices), current drive calculations require a careful consideration of the supra-thermal electrons. Since the relativistic effects behave rather differently from the collisional effects (i.e. their weight increases with the temperature), it is possible for high-temperature plasmas to apply the relativistic model in the collisionless limit. Relativistic considerations with parallel momentum conservation (*pmc*) for the different current drive mechanisms were given in Refs. 25–27, 30.

In the present work, recent progress in electron cyclotron current drive calculations is reviewed. A comparative analysis of the different approaches and their applicabilities is presented. Considering various ITER scenarios and calculating ECCD with the different models implemented in the ray-tracing code TRAVIS [31], the role of parallel momentum conservation in like-particle collisions is illustrated. The applied models have been benchmarked against other ray-tracing codes [28] as well as the Fokker-Planck code CQL3D [12].

II. ADJOINT TECHNIQUE

A. General definitions

In the ray-tracing codes, the toroidal current driven on the elementary arc-length of the ray-trajectory can be calculated. The key value is the current drive efficiency,

$$\eta = \left\langle j_\parallel \right\rangle / \left\langle p_{\rm abs} \right\rangle , \qquad (1)$$

where $\left\langle j_\parallel \right\rangle$ is the density of generated current and $\left\langle p_{\rm abs} \right\rangle$ the density of the absorbed power, which are the functions only of the flux-surface label (here, $\langle A \rangle = \int A \frac{dl}{B} / \int \frac{dl}{B}$ denotes averaging over the magnetic surface). In the linear approach, which is assumed to be valid in the ray-tracing calculations, the efficiency does not depend on the absorbed power. (For details related to the practical calculation of the total toroidal current in the ray-tracing codes we refer to the Appendix.)

Apart from the direct calculation of current drive from the solution of the Fokker-Planck equation, the easiest way to calculate the efficiency is with the adjoint technique. This technique is well described in the literature and, apart from notation, we follow in this chapter the line of Refs. 6 and 7. Since the drift trajectory of particles in the conventional neoclassical ordering is assumed to remain on the magnetic-flux surface, we represent the electron distribution function in the variables $(s, \mathbf{u})$, where s characterizes the position of a particle trajectory on the magnetic-flux surface and $\mathbf{u} = (u, \xi)$ is momentum per unit mass, $u = v\gamma$ with $\gamma = \sqrt{1 + u^2/c^2}$, and pitch, $\xi = u_\parallel/u$ with $u_\parallel = \mathbf{u} \cdot \mathbf{B}/B$. The normalized magnetic moment, $\lambda = (1 - \xi^2)/b$, will also be used when convenient (here, $b = B/B_{\rm max}$ with $B_{\rm max}$ the maximum value of magnetic field on the given magnetic surface). Note

also that the relativistic formulation is applied throughout the paper despite the fact that in some cited papers only the non-relativistic model has been considered.

The current driven by the RF source, $j_\parallel = -e\int \mathrm{d}^3u\ v_\parallel \delta f_e$, can be formally calculated by solving the linearized drift kinetic equation, which describes the linear response of electrons to the RF source,

$$v_\parallel \nabla_\parallel \delta f_e - C^{\mathrm{lin}}(\delta f_e) = Q_{\mathrm{RF}}(f_{eM}) \equiv -\frac{\partial}{\partial \mathbf{u}} \cdot \mathbf{\Gamma}_{\mathrm{RF}}(f_{eM}), \tag{2}$$

where $\nabla_\parallel \equiv \partial/\partial l$ is the derivative along the field-line (for the considered problem, the drifts which are not along $\mathbf{B}$ can be neglected), $\delta f_e \equiv f_e - f_{eM}$ is the distortion of the electron distribution function from the Maxwellian, $f_{eM} = \mu n_e/[4\pi c^3 K_2(\mu)] \cdot \mathrm{e}^{-\mu\gamma}$ with $\mu = m_{e0}c^2/T_e$ and K_2 the McDonald's function, $C^{\mathrm{lin}}(\delta f_e)$ is the linearized collision operator and $\mathbf{\Gamma}_{\mathrm{RF}} = -\mathsf{D}_{\mathrm{RF}} \cdot \partial f_{eM}/\partial \mathbf{u}$ is the quasi-linear diffusion flux in $\mathbf{u}$-space.

Let us consider also the adjoint kinetic equation,

$$v_\parallel \nabla_\parallel (\chi f_{eM}) + C^{\mathrm{lin}}(\chi f_{eM}) = -\nu_{e0}\ \frac{v_\parallel}{v_{\mathrm{th}}}\, b\, f_{eM}, \tag{3}$$

where $\chi(-u_\parallel)$ is formally identical (apart from normalization) to the generalized Spitzer function in toroidal geometry, i.e the distribution function in a weak dc "parallel" electric field [17, 18, 21]. (Here, we follow the terminology employed in the literature devoted to current drive and refer to the steady state solution of the adjoint kinetic equation, $\chi(s,\mathbf{u})$, as the Green's function which, actually, was introduced for the dynamic problem [19, 20].) Then, substituting $(v_\parallel B)$ from Eq. (3) in the definition of $j_\parallel$ and exploiting the self-adjoint properties of the Vlasov and collision operators,

$$\left\langle \int \mathrm{d}^3u\, \frac{f}{f_{eM}} \begin{bmatrix} V(g) \\ C^{\mathrm{lin}}(g) \end{bmatrix} \right\rangle = \left\langle \int \mathrm{d}^3u\, \frac{g}{f_{eM}} \begin{bmatrix} -V(f) \\ C^{\mathrm{lin}}(f) \end{bmatrix} \right\rangle \tag{4}$$

(here, $V = v_\parallel \nabla_\parallel$), it is possible to express the current drive through the convolution of the RF source with $\chi(s,\mathbf{u})$. Since $\nabla \cdot (j_\parallel \mathbf{B}/B) = 0$, which follows directly from Eq. (2), $j_\parallel/B = \langle j_\parallel\rangle/\langle B\rangle = \langle j_\parallel B\rangle/\langle B^2\rangle$ is a function of only the flux-surface label, the final expression for the current drive can be written as follows [6, 7, 16, 23, 24]:

$$\langle j_\parallel \rangle = -\frac{e v_{\mathrm{th}}}{\nu_{e0}} \cdot \frac{\langle b\rangle}{\langle b^2\rangle} \cdot \left\langle \int \mathrm{d}^3u\ \chi Q_{\mathrm{RF}}(f_{eM}) \right\rangle, \tag{5}$$

where $\nu_{e0} = 4\pi n_e e^4 \ln\Lambda/(m_{e0}^2 v_{\mathrm{th}}^3)$ is the collision frequency for the thermal electrons. Since no additional assumption was made, the expression for the driven current Eq. (5) is general and applicable for any configuration and arbitrary collisionality. The limitation is only the validity of the linear approach and of the neoclassical ordering.

Finally, since the local density of absorbed power is $p_{\mathrm{abs}} = \int \mathrm{d}^3u\ m_{e0}c^2(\gamma-1)Q_{\mathrm{RF}}$, the efficiency can be expressed as

$$\eta = -\frac{e v_{\mathrm{th}}}{m_{e0}\nu_{e0}} \cdot \frac{\langle b\rangle}{\langle b^2\rangle} \cdot \frac{\left\langle \int \mathrm{d}^3u\ \frac{\partial \chi}{\partial \mathbf{u}} \cdot \mathbf{\Gamma}_{\mathrm{RF}} \right\rangle}{\left\langle \int \mathrm{d}^3u\ \frac{\mathbf{u}}{\gamma} \cdot \mathbf{\Gamma}_{\mathrm{RF}} \right\rangle}. \tag{6}$$

Being quite convenient for numerical representation, this form is the usual basis for ECCD calculations in the ray-tracing codes.

Here, we do not specify the quasi-linear diffusion coefficient D_{RF} (it is assumed only that this term is known). It should be sufficient to say only that due to a high localization in phase space (in ray-tracing, $\mathsf{D}_{\mathrm{RF}} \propto \delta(\gamma - n\omega_{ce}/\omega - N_\parallel u_\parallel/c)$ along the given ray), knowledge of the complete $\chi(s,\mathbf{u})$ is necessary (contrary to calculation of conductivity and bootstrap current, where only the 1st Legendre moment of the response function is required).

Since conservation of energy in the linearized collision operator, $C^{\mathrm{lin}}(g) \equiv C_{ee}(g; f_{eM}) + C_{ee}(f_{eM}; g) + C_{ei}(g; f_{iM})$, is of minor importance for the Spitzer problem, it is sufficient to keep only the 1st Legendre harmonic of g in the integral term, i.e. $C_{ee}(f_{eM}; g) \simeq \xi C_{ee,1}(f_{eM}; g_1)$ with $g_1 = \frac{3}{2}\int_{-1}^{1} g\xi \mathrm{d}\xi$ (here and below, we use, following Ref. 6, the notation $C[f(u)P_n(\xi)] = P_n(\xi)C_n[f(u)]$). Apart from this, the collisions with ions can be considered in the limit $m_i/m_e \to \infty$ with only the pitch-scattering taken into account, i.e. $C_{ei}(g; f_{iM}) \simeq \nu_{ei} L g$ with $L = \frac{1}{2}\frac{\partial}{\partial\xi}(1-\xi^2)\frac{\partial}{\partial\xi}$.

In order to consider this problem in a proper way, attention must be focused on the interplay of geometrical effects (magnetic configuration) and the collisional response, which are described by the Vlasov and collision operators, respectively. To date, there are no tools for precisely solving the generalized Spitzer problem Eq. (3) in arbitrary magnetic configurations which can be routinely applied for ECCD. Instead, the problem is reduced to a solvable level by simplifying assumptions which do not necessarily hold under experimentla conditions.

B. Collisional (classical) limit

In Eq. (3), different time-scales exist: while the first term (Vlasov operator) is characterized by the transit time τ_t, i.e. $v_\parallel \nabla_\parallel \propto \tau_t^{-1}$, the collision operator is characterized by the collision time τ_c, i.e. $C^{\mathrm{lin}} \propto \tau_c^{-1}$. For ordering Eq. (3), we take into account that the ratio of $\tau_t/\tau_c \equiv \nu_e^* = \nu_e(u)\gamma R/\iota u$ can vary significantly.

When collisionality is very high, $\nu_e^* \gg 1$, i.e. $\tau_t \gg \tau_c$, Eq. (3) reduces to the local problem with the straight magnetic field (formally, the 1st term in Eq. (3) becomes negligible). In this case, only the 1st Legendre harmonic of χ is necessary, i.e. $\chi = \xi\chi_1(u)$ and $\chi_1 = \frac{3}{2}\int_{-1}^{1}\chi\xi\mathrm{d}\xi$. Then, instead of Eq. (3), it becomes sufficient to solve the 1D integro-differential equation for χ_1,

$$\widehat{C}_1^{\mathrm{lin}}(\chi_1) = -\nu_{e0}\,\frac{u}{\gamma v_{\mathrm{th}}}. \tag{7}$$

Here, $\widehat{C}_1^{\rm lin}(\chi_1) \equiv C_1^{\rm lin}(\chi_1 f_{eM})/f_{eM}$ with $C_1^{\rm lin}$ is the 1st Legendre harmonic of the linearized collision operator. This is the classical Spitzer problem for calculation of the plasma conductivity which has been thoroughly studied for both non-relativistic [17, 18] and relativistic [21] approaches (apart from the normalization, χ_1 coincides with the classical Spitzer function). This gives the upper limit for current drive (CD) efficiency, but is of no practical relevance for hot plasmas in toroidal devices.

C. Low collisionality (long-mean-free-path) limit

In the opposite (low collisionality or "collisionless") limit, $\nu_e^* \ll 1$, i.e. $\tau_t \ll \tau_c$, the impact of the trapped particles is important. In this case, the dimensionality of the problem can also be reduced to 2D since the spatial dependence appears only due to the coupling between the pitch, $\xi = \sigma\sqrt{1-\lambda b}$ with $\sigma = \pm 1$, and the local magnetic field, $b(s)$, through the (normalized) magnetic moment, λ. By averaging Eq. (3) over the magnetic surface, the Vlasov operator is annihilated and the problem is reduced to a 2D equation [6, 7],

$$\left\langle \frac{b}{|\xi|}\,\widehat{C}^{\rm lin}(\chi)\right\rangle = -\sigma\nu_{e0}\,\frac{u}{\gamma v_{\rm th}}\,\langle b^2\rangle. \qquad (8)$$

This is the basic model for calculation of CD in the different ray- and beam-tracing codes. The form chosen for the collision operator is very important for the solution. Note also that in this approach the problem is antisymmetric (with respect to ξ), and, as a consequence, only the antisymmetric part of the quasi-linear operator contributes in the current drive calculated by the convolution Eq. (5).

Expressing the Lorentz operator as $\hat{L} = 2|\xi|/b \cdot \partial/\partial\lambda(\lambda|\xi|\partial/\partial\lambda$, the general solution of Eq. (8) in the variables $(u,\lambda;\sigma)$ can be represented, similar to Ref. 27, as a series

$$\chi^{(e)}(u,\lambda;\sigma) = \sigma\sum_{k=odd}\mathcal{F}_k(u)\mathcal{P}_k(\lambda) \qquad (9)$$

(in order to distinguish this exact solution from the other approximations, considered below, we mark it by the index e), where $\mathcal{P}_k$ are the eigenfunctions of the operator

$$2\left\langle\frac{b}{|\xi|}\right\rangle^{-1}\cdot\frac{\partial}{\partial\lambda}\lambda\langle|\xi|\rangle\frac{\partial\mathcal{P}_k}{\partial\lambda} + A_k\mathcal{P}_k = 0. \qquad (10)$$

For the problem considered, the eigenfunctions $\mathcal{P}_k(\lambda)$ are defined for $\lambda \le 1$, i.e. only for the passing particles, and satisfy the boundary conditions $\mathcal{P}_k(0) = 1$ and $\mathcal{P}_k(1) = 0$ (actually, these boundary conditions select the "odd" modes making the set of eigenfunctions antisymmetric with respect to pitch). Practically, it is the same as bounce-averaging which actually was applied in Ref. 27, where the pitch at the minimum of B, $\xi_0 = \sigma\sqrt{1-\lambda b_{\rm min}}$, instead of λ was used as a variable. (In Ref.32, where a similar idea was used for solving the problem of fast-ion slowing down, the features of the eigenfunctions $\mathcal{P}_k$ considered as functions of ξ_0 were analytically studied in detail for circular tokamaks.)

Due to this expansion, the problem is reduced to a set of 1D integro-differential equations for $\mathcal{F}_k(u)$, which can be easily solved numerically. In Ref. 27, this system is solved, similar to Ref. 15, by the variational principle, where instead of a polynomial fit the spline technique is applied, which gives a much more accurate solution. Since the series in Eq. (9) converges rapidly (in practice, only several odd harmonics are necessary), this method can be easily applied for ECCD calculations. Being originally developed only for circular tokamaks, the numerical model was revised recently to make it applicable for arbitrary magnetic configurations. (In order to distinguish it from others used below, we refer to this model by the name of the original code where it was firstly applied, i.e. SYNCH [27]. This model is presently implemented in the TRAVIS code as an option.)

Apart from this exact solution, it is possible also to simplify Eq. (8) without significant loss of accuracy. Since the pitch-scattering of electrons is the dominating process, all terms in the collision operator apart from the Lorentz term can be approximated by only the first Legendre harmonic [5–7],

$$\widehat{C}^{\rm lin}(\chi) \simeq \nu_e(u)\hat{L}(\chi) + \xi\left(\widehat{C}^{\rm lin}_{ee,1}(\chi_1) + \nu_{ee}(u)\chi_1\right), \qquad (11)$$

where $\widehat{C}^{\rm lin}_{ee,1}$ is the first Legendre harmonic of the linearized e/e collision operator. In this approximation, Eq. (8) can be solved analytically [6, 7],

$$\begin{aligned}
\chi^{(a)}(u,\lambda;\sigma) &= \sigma\mathcal{H}(\lambda)\,K(u),\\
\mathcal{H}(\lambda) &= \frac{\langle b^2\rangle}{2f_c}\,h(1-\lambda)\int_\lambda^1\frac{d\lambda}{\langle\sqrt{1-\lambda b}\rangle},\\
f_c = 1 - f_{\rm tr} &= \frac{3}{4}\langle b^2\rangle\int_0^1\frac{\lambda d\lambda}{\langle\sqrt{1-\lambda b}\rangle},
\end{aligned} \qquad (12)$$

where f_c and $f_{\rm tr}$ are the fractions of circulating and trapped particles, respectively, and $h(x)$ is the Heaviside function. (The label of the solution, $\chi^{(a)}$, is used here to indicate that an approximation has been made.) The function $K(u) = \frac{3}{2}\int_0^1 d\lambda\,\chi^{(a)}(u,\lambda;\sigma=1)$, which is proportional to the Spitzer function, must be found as the solution of a 1D integro-differential equation [6, 7],

$$\widehat{C}_1^{\rm lin}(K) - \frac{f_{\rm tr}}{f_c}\,\nu_e(u)K(u) = -\nu_{e0}\,\frac{u}{\gamma v_{\rm th}}. \qquad (13)$$

In this approach, only the antisymmetrical part of the quasi-linear operator can contribute in the convolution Eq. (5) which gives the driven current. Nevertheless, when applied only to the collisionless limit, this approach is sufficiently accurate.

Most important for a precise calculation of ECCD is the model chosen for the operator $\widehat{C}^{\rm lin}$. Generally, the model includes the diffusion over velocity and drag

of the test-particle in the Maxwellian background, the pitch-angle scattering, and the reaction coming from the Maxwellian which guaranties parallel momentum conservation. In this case, the first Legendre harmonic of the relativistic collision operator, $\widehat{C}_1^{\rm lin}$, necessary for solving Eq. (13) can be written as follows [6]:

$$\begin{aligned}\widehat{C}_1^{\rm lin}(K) &= \frac{1}{u^2}\frac{d}{du}\left(u^2 D_{uu}^{e/e}\frac{dK}{du}\right) + F_u^{e/e}\frac{dK}{du} \\ &- \nu_e K + I_{ee}(K).\end{aligned} \tag{14}$$

Here, $D_{uu}^{e/e}$ and $F_u^{e/e}$ are diffusion over velocity and friction Coulomb coefficients, respectively, calculated for the Maxwellian background, and $I_{ee}(K) = C_{ee,1}(f_{eM};K)/f_{eM}$ is the first Legendre harmonic of the integral part of the collision operator, which is responsible for parallel momentum conservation in e/e-collisions (all the necessary definitions are in Ref. 21). This model (here and below, this approach with parallel momentum conservation is abbreviated as the *pmc* model) is most useful and correct for calculation of current drive in the various scenarios.

Recently, using the approximate solution of Eq. (12), $\chi^{(a)}$, a very fast and sufficiently accurate numerical model for calculating the ECCD efficiency was developed [30] (below, we refer to this model by name of the code for which it has been developed, i.e. TRAVIS). This model is based on the solution of the integro-differential equation Eq. (13) with the collision operator Eq. (14), where the Spitzer function, $K(u)$, is calculated with parallel momentum conservation in the e/e collisions. In order to simplify and accelerate the numerical solution, relativistic effects are taken into account through a power expansion in $\mu^{-1} = T_e/m_{e0}c^2$ (in fact, it is a weakly relativistic approach) and for practical applications it is completely sufficient to truncate the expansion at the term $\propto \mu^{-2}$). To numerically solve Eq. (13), the variational principle [15, 33] was applied and the solution is defined as the minimum of the relativistic functional through a polynomial fit (for details, see Ref. 30). This solver has been successfully implemented and tested in the ray-tracing code TRAVIS and is now routinely used for ECCD calculations [29, 34–37]. Apart from this, this solver is also in use for current drive calculations in scenarios with electron Bernstein waves in TJ-II stellarator [38].

1. *High-speed limit*

Historically, the high-speed-limit (*hsl*) approach [3, 5, 7] was commonly accepted as the standard for calculation of ECCD. This approach is based on the assumption that only the supra-thermal electrons with $\mu(\gamma-1) \gg 1$ (or, simply, $u \gg v_{\rm th}$) are involved in the cyclotron interaction. Since for supra-thermal electrons, the e/e drag and the pitch-angle scattering are dominant while the contribution from the diffusion term in momentum space and the integral term responsible for the parallel momentum conservation are negligible, the collision operator Eq. (14) can be significantly simplified:

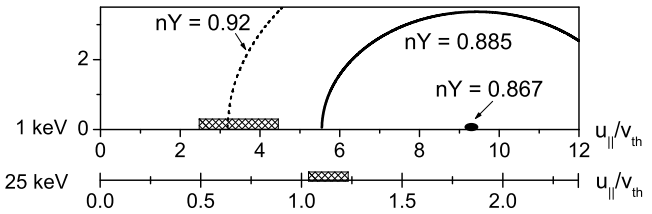

FIG. 1: The cyclotron resonance lines in momentum space $(u_\parallel, u_\perp)$ for $N_\parallel = 0.5$, $nY = 0.885$ (solid line) and $nY = 0.92$ (dashed line) are shown (here, $nY \equiv n\omega_{ce}/\omega$). The axis is scaled for the different electron temperatures: $T_e = 1$ keV (upper axis) and $T_e = 25$ keV (lower axis). Also the ranges of the main contribution in absorption are marked by the pattern along the abscissa.

$$\widehat{C}_1^{\rm hsl}(K) \simeq F_u^{e/e}\frac{dK}{du} - \nu_e K. \tag{15}$$

Estimating then for $u \gg v_{\rm th}$ the necessary Coulomb coefficients as

$$\begin{aligned}\nu_e(u) &\simeq \nu_{e0}\,\frac{\gamma v_{\rm th}^3}{u^3}\,(1+Z_{\rm eff}), \\ F_u^{e/e}(u) &\simeq -\nu_{e0}\frac{\gamma^2 v_{\rm th}^3}{u^2},\end{aligned} \tag{16}$$

the analytical *hsl*-solution of Eq. (13) can be found [7],

$$K^{hsl}(u) = \frac{1}{v_{\rm th}^4}\left(\frac{\gamma+1}{\gamma-1}\right)^{\hat\rho}\int_0^u {\rm d}u'\left(\frac{u'}{\gamma'}\right)^3\left(\frac{\gamma'-1}{\gamma'+1}\right)^{\hat\rho}, \tag{17}$$

where $\hat\rho = (1+Z_{\rm eff})/2f_c$. Due to its simplicity for numerical calculations, this approach was implemented in many ray- and beam-tracing codes (see Ref. 28 and the references therein) and successfully applied for simulation of the various ECCD scenarios. Unfortunately, in high-temperature plasmas, the energy range of electrons which make the main contribution to ECCD is not so far from the bulk, and the *hsl* approach fails even for highly oblique launch.

To illustrate this, let us consider a simplified scenario with X-mode, 2nd harmonic, constant T_e and with increasing B along the ray with $N_\parallel = 0.5$. In Fig. 1, the cyclotron resonance lines, $\gamma = N_\parallel u_\parallel/c + nY$ (here, $Y \equiv \omega_{ce}/\omega$ and $n = 2$), are shown on the plane $(u_\parallel, u_\perp)$ for $nY = 0.885$ (solid line) and $nY = 0.92$ (dashed line). The axis is scaled for two electron temperatures, 1 keV (upper axis) and 25 keV (lower axis). Starting from $nY = 0.867$ (thick point), the resonance interaction appears, but actually the absorption becomes significant for somewhat higher values of nY. Let us first look at the case $T_e = 1$ keV. Assuming that the density is sufficiently high to make the plasma optically thick, the main contribution to the absorption is around the line with $nY = 0.92$ (dashed line) where electrons not so far from the bulk become involved in the cyclotron interaction.

The corresponding deposition range ($u/v_{\rm th} \sim 2.5 - 4$) is marked by the pattern at the upper axis. In this case, the *hsl* approach is marginally applicable. Considering then the same resonance for $T_e = 25$ keV, one finds that the resonance interaction starts practically within the bulk ($u/v_{\rm th} \simeq 1.8$) and the power will be absorbed completely much closer to the point where the resonance appears, i.e within the narrow layer around $nY = 0.885$ (solid line) where the electrons with $u/v_{\rm th} \sim 1$ produce the main contribution to absorption. In this case, taking into account parallel momentum conservation is mandatory.

2. *Solution of Spitzer problem in different approaches*

In Fig. 2, the solutions of Eq. (13) obtained in the different approaches are shown. The calculations were performed for a circular tokamak with a magnetic field $B = B_0/(1 + \epsilon\cos\theta)$ and $\epsilon = r/R_0 = 0.2$ (here, θ is the poloidal angle). In order to illustrate the weight of relativistic effects, a temperature typical for ITER is used, $T_e = 25$ keV. Both exact, $\chi^{(e)}$, and approximate, $\chi^{(a)}$, solutions (Eq. (9) and Eq. (12), respectively) were used for calculations. Apart from this, the approximate solution was used in three different approaches, weakly relativistic and non-relativistic polynomial fit, as well as the fully relativistic *hsl*.

Comparing the non-relativistic and the relativistic solutions shown in Fig. 2, one finds that for 25 keV relativistic effects are significant. This means that the non-relativistic *pmc*-solvers developed in the Refs. 6, 33 have a very limited applicability (practically, only for $T_e < 1$ keV). It is found also that the discrepancy between the numerical *pmc*-solutions, obtained by the solvers TRAVIS (approximate solution $\chi^{(a)}$) and SYNCH (exact solution $\chi^{(e)}$), is rather small in this range (this discrepancy is the fault of the rather simple trial function chosen in Refs. 15, 30 for fitting and is not due to the weakly relativistic approach itself).

The most important result is that in the range $u < 4v_{\rm th}$, which is predominant for driving the current, *pmc*-solutions significantly exceed the *hsl*-solution. Note that contrary to the transport theory, where the current is completely defined by $\langle\chi_1\rangle$, i.e the first Legendre harmonic of χ averaged over the flux surface (see Ref. 39 and the references therein), the ECCD efficiency, η, is much more sensitive to the local behavior of χ. Indeed, as follows from Eq. (6), η is defined not by χ itself but rather by the projection of the χ-gradient onto the quasi-linear flux in momentum space. Formally, since the pitch-dependence of χ defined by the function $\mathcal{H}(\lambda)$ in Eq. (12) is the same for both *hsl*- and *pmc*-approaches, *hsl* may lead (formally) not only to underestimation of the local ECCD efficiency but even to overestimation of it depending on the resonance condition. In practice, nevertheless, for realistic scenarios, the current drive calculated in the *hsl*-approach tends to be underestimated.

It is useful to mention here also that both the *hsl* and *pmc* models have the same "pitch"-dependence, while the $u-$dependence is different (see Eq. (9) and Eq. (12)). Since the current drive efficiency in Eq. (6) is actually defined by the dot-product $\partial\chi/\partial\mathbf{u}\cdot\mathbf{\Gamma}_{\rm RF}$, the difference between the *hsl*- and *pmc*-approaches is strongly pronounced only if $\partial\chi/\partial u$ becomes dominant.

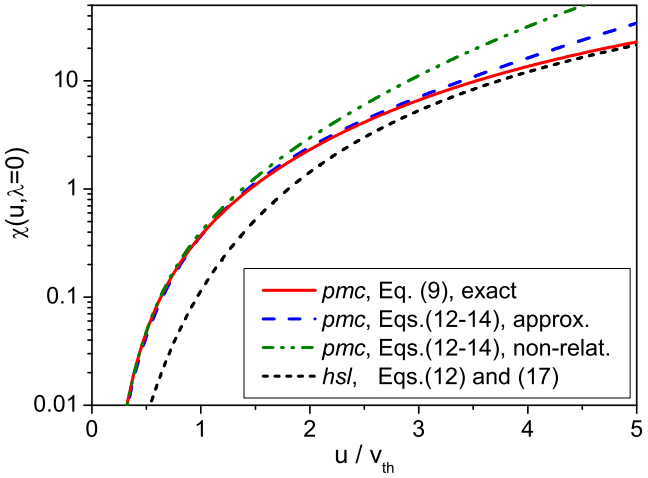

FIG. 2: (Color online) Spitzer function, calculated with different approaches for circular tokamak with $\epsilon = 0.2$. Plasma parameters $T_e = 25$ keV and $Z_{\rm eff} = 1$. Exact fully relativistic solution is calculated by solver SYNCH. All other approximate solutions (fully-relativistic *hsl*, weakly-relativistic and non-relativistic polynomial fit) are calculated by TRAVIS.

III. LOCAL ECCD EFFICIENCY IN TOKAMAKS

For comparison of the considered approaches, the local dimensionless ECCD efficiency, $\zeta^* = (e^3/\varepsilon_0^2)(n_e/T_e)\langle j_\parallel\rangle/2\pi\langle p_{\rm abs}\rangle$ (here, we use the definition and notation from Eq. (10) in Ref. 7), is calculated for X-mode, 2nd harmonic with the different values of $N_\parallel = 0.34$, 0.42 and 0.5 (which correspond to the different launch angles 20°, 25° and 30° measured from the perpendicular to the magnetic field, respectively) in the same circular tokamak as above. The plasma parameters, $n_e = 2\times10^{19}$ m^{-3}, $T_e = 5$ keV and $Z_{\rm eff} = 1$, are chosen in such a way that the main contribution in current drive is generated by electrons with $u \sim 2v_{\rm th}$, where parallel momentum conservation starts to be important.

In Fig. 3, the local ECCD efficiency is plotted as a function of the normalized magnetic field, $nY = n\omega_{ce}/\omega$, which actually defines the location of the resonance line in the phase space for the given $N_\parallel$. The calculations were performed for two spatial points with poloidal angles $\theta = 0$ and $\theta = 180°$, i.e. for the minimum of B (a) and the maximum of B (b), respectively, on the same magnetic surface, $\epsilon = 0.2$. In the figures, only the case $nY < 1$ is shown, where only the electrons with $k_\parallel v_\parallel > 0$

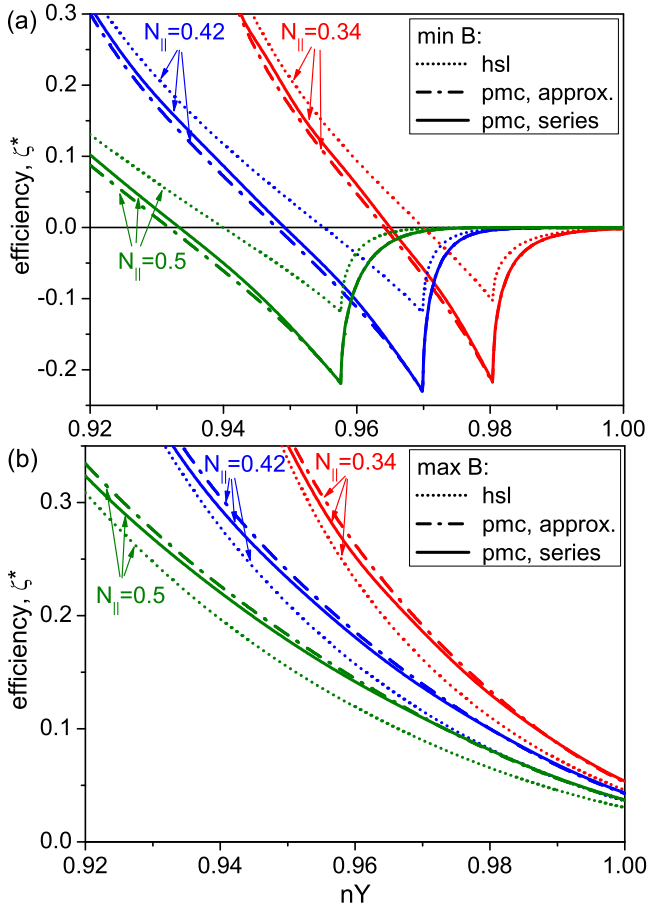

FIG. 3: (Color online) Dimensionless ECCD efficiency for X2-mode, calculated for different $N_\parallel$ as function of normalized magnetic field, $nY = n\omega_{ce}/\omega$, with different approaches for circular tokamak. Plasma parameters: $n_e = 2 \times 10^{19}\mathrm{m}^{-3}$, $T_e = 5$ keV, $Z_{\mathrm{eff}} = 1$. For the same magnetic surface, $\epsilon = 0.2$, calculations were performed for two points, which correspond to minB (a) and maxB (b).

contribute in generation of the current. In the opposite case (not shown), with $k_\parallel v_\parallel < 0$, when both $v_\parallel > 0$ and $v_\parallel < 0$ belong to the same resonance line, the Fisch-Boozer current is generated in both directions, partly annihilating itself. This case, which can be met only in tenuous or at least optically gray plasmas, is not of interest for ECCD scenarios.

One can see in both Fig. 3 (a) and (b) that the local ECCD efficiency, ζ^*, calculated with the *hsl* model, significantly differs from the *pmc* values. This is the most important result of this paper. Note also that ζ^* calculated by both exact and approximate *pmc* models are in satisfactory agreement. The small discrepancy arises from the choice of the trial function for fitting the solution in the approximate solution of Eq. (13), which is too simple to accurately cover the complete velocity range. As a consequence, the exact *pmc* model gives a somewhat better convergence to the *hsl* model in the range of lowest nY values, where only supra-thermal electrons contribute in ECCD (see also Fig. 2). In practice, nevertheless, the resonance line for these values of nY is situated sufficiently far from the bulk (see also Fig. 1), where the absorption is negligible, and this discrepancy does not produce any significant error in calculation of the current drive profile and the total current.

The efficiency calculated for the minimum of B (see Fig. 3(a)) decreases with increasing of the magnetic field and changes sign well before the point $nY = 1$, where the resonance line in velocity space crosses the axis $v_\parallel = 0$. This effect (inverting of the sign) is induced by the trapped particles and is called the Ohkawa effect (see, e.g. Ref. 5, 6). Strictly speaking, this behavior is induced by influence of the trapped/passing boundary in the collisional response described by the Green's function and not by the quasi-linear diffusion of the passing electrons into the trapped domain itself, as was assumed by Ohkawa [1]. Actually, the effect originally proposed by Ohkawa appears only when the resonance line crosses the passing/trapped boundary. In Fig. 3(a), one can see that the slope of the efficiency at this point sharply changes sign and rapid dropping of the efficiency appears. This happens since the trapped electrons absorb the power but do not contribute to the current. Here, we follow the terminology already employed in the literature and also refer to this general influence of the trapped particles as the Ohkawa effect.

It is important to mention here also that the *hsl* model can both underestimate and overestimate the local value of CD efficiency (see Fig. 3(a)), depending on the chosen conditions. But being weighted by the deposition profile, which practically nullifies the contribution from the supra-thermal electrons, the total CD efficiency calculated by the *hsl* model is, as shown in the section IV, almost always (apart from high launch angles) underestimated. In the case of highly oblique prapagation of the RF beam in optically thick plasmas, the deposition profile nullifies also the contribution from the bulk, making the difference between the approaches small.

IV. BENCHMARKING OF THE MODELS: ECCD IN ITER

The practical importance of performing accurate calculations of the current drive can be illustrated for quite typical ECCD scenarios in ITER. In Fig. 4(a), the results of ray-tracing calculations for the ITER reference scenario-2 are presented, where the angle-scan for the equatorial launcher (top-mirror) is depicted. Three different codes were applied, TORAY-GA (Ref. 40) with *hsl*-model, TRAVIS (both *hsl*- and *pmc*-models) and the Fokker-Planck code CQL3D. For calculations by TRAVIS, both "exact" and "approximate" numerical solvers were applied, which are based on the fully relativistic splining and the weakly relativistic polynomial fit, respectively.

One can see in Fig. 4(a), that the results obtained by both TORAY-GA and TRAVIS with the same *hsl* approach applied are in perfect agreement. On the other hand, a

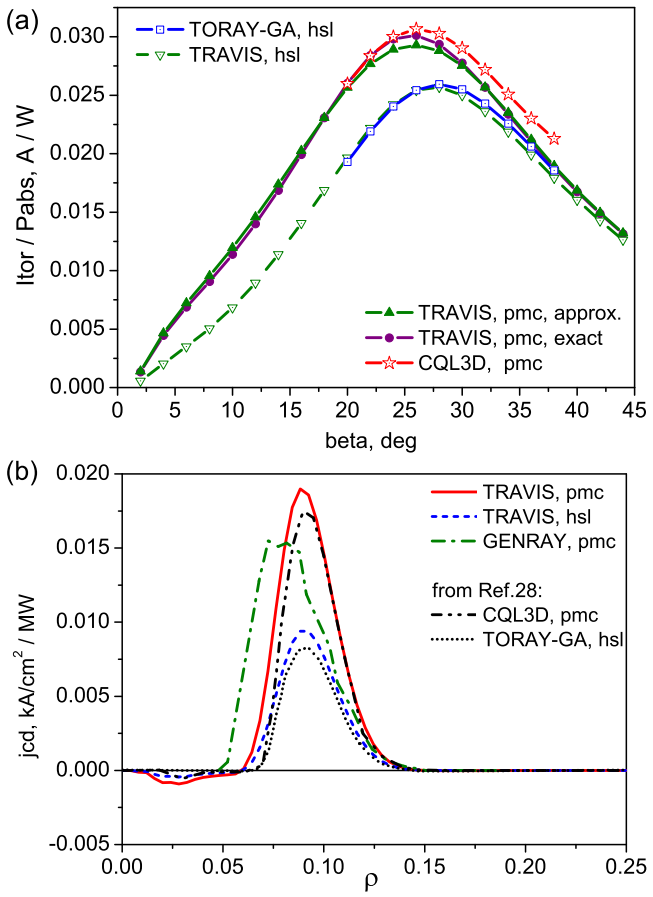

FIG. 4: (Color online) ECCD efficiency as function of the toroidal launch angle for ITER, equatorial launcher, top mirror (a), and the ECCD profiles obtained in a *gedankenexperiment* for ITER [28] (b), by different codes using different approaches. Toroidal current drive calculated in *gedankenexperiment*: TRAVIS - 25.4 kA/MW for *pmc* and 12.6 kA/MW for *hsl*; GENRAY (*pmc*) - 25.8 kA/MW; CQL3D (*pmc*) - 24.0 kA/MW [28]; TORAY-GA (*hsl*) - 11.62 kA/MW [28].

comparison with the results obtained with the *pmc* model shows that the *hsl* model significantly underestimates the ECCD efficiency (especially for small and moderate angles) and the convergence with *pmc* results is observed only for very high obliqueness. For the angles which are of the main interest, i.e. for the toroidal launch angle $\beta = 20^\circ - 40^\circ$, the discrepancy between the *hsl* and *pmc* models varies from 10% to 30%. This is not surprising given the previous considerations stated previously.

From comparison of results obtained by TRAVIS with the *pmc*-model and by CQL3D shown in Fig. 4(a), one finds that these results also coincide well. As the most important consequence of this benchmark, it can be pointed out that the accuracy of the *pmc*-model is well confirmed by Fokker-Planck calculations. Indeed, despite the slight discrepancy of the results at the large angles, where the Fokker-Planck results do not converge to the *hsl* values (this can be explained by the different representation of the quasi-linear term in the ray-tracing and the Fokker-Planck codes, and, additionally, by accumulation of discrepancies induced by different numerical representations due to the long ray-trajectory for large angles), the qualitative and quantitative agreement is sufficiently high.

As an additional and transparent test of the role of parallel momentum conservation, in Ref.28 the *gedankenexperiment* was proposed with a moderate launch angle (12.3° from radial) just to make the bulk electrons responsible for absorption. Additionally, the magnetic field was scaled in order to locate the electron cyclotron resonance quite close to the axis, where the trapped-particles fraction is small (the friction of passing electrons with trapped ones can significantly mask the effect of parallel momentum conservation). By simulations, it was found that the *hsl* model in several different codes underestimates the total current by a factor of two in comparison with the Fokker-Planck calculations. These results are shown and discussed in Fig. 12 in Ref. 28. The reason for such a strong underestimate of the ECCD with the *hsl* model is that the electrons with $u_{\rm res} \sim 1.5 v_{\rm th}$ are responsible for the current drive which clearly violate the applicability of the *hsl* model. Furthermore, Fokker-Planck calculations even without parallel momentum conservation show clearly that also diffusion over velocity, which is neglected in the *hsl* model (compare Eq. (14) and Eq. (15)), plays an important role. For reference, these results are partly reproduced here also in Fig. 4(b).

The same scenario has been recalculated by the TRAVIS code with both *pmc* and *hsl* models (see Fig. 4(b)). It must be mentioned here that despite qualitative agreement and approximately the same toroidal current, the current drive profile calculated for the parameters from Ref. 28 is slightly shifted by $\delta\rho \simeq 0.02$. (The best candidate for explanation is the different representations and accuracy of the equilibrium in the codes.) In order to have a similar location of the current profile as shown in Fig. 12 of Ref. 28, the magnetic field here was slightly "corrected" by 0.5%, i.e. instead of 5.63 T as originally was applied, the value $B = 5.6$ T was used. At the same time, since plasma parameters are practically constant near the axis, the shift of the $\langle j_\parallel \rangle(\rho)$ profile being sufficiently small does not produce any significant effect and the total toroidal current is practically the same. In calculations, both exact and approximate models (Eq. (9) and Eq. (12), respectively) were applied, but the results obtained are practically indistinguishable.

As expected, the results from the *hsl* model are very similar to other ray- and beam-tracing calculations from [28], while the results from the *pmc* model agrees well with the results from the Fokker-Planck code. Apart from this, the same scenario was simulated recently by the GENRAY code [41] which has already implemented the numerical package [25, 42] for calculation of the Green's function with parallel momentum conservation. The latter is also shown in Fig. 4 (b) and both the shape and the value of the current are quite similar to other

pmc calculations. All results obtained here confirm the conclusion that the *pmc* model is mandatory for simulations of ECCD scenarios in high temperature plasmas.

V. SUMMARY

In this paper, a description of the different approaches necessary for calculations of the electron cyclotron current drive in plasmas with low collisionality has been presented. All the formulations based on the adjoint technique are oriented for usage in ray- and beam-tracing codes, which at the present time are the main tools for numerical studies of ECRH and ECCD physics. The main attention was focused on parallel momentum conservation in the like-particle collisions which is much more precise for calculations of ECCD than the high-speed-limit (especially in hot plasmas). It was shown that an accurate kinetic solution of the Spitzer problem with parallel momentum conservation in like-particle collisions is of high importance in ECCD physics and may give a significant effect.

In order to make it applicable for practical calculations, simple and fast numerical solvers have been developed recently to solve the Spitzer problem in the collisionless limit with parallel momentum conservation in the e/e collisions. These solvers cover the desired range of applicability well and are suitable for arbitrary 3D magnetic configuration. These solvers have been implemented in the ray-tracing code TRAVIS and successfully benchmarked against the Fokker-Planck code for ITER scenarios. It was shown that the model with parallel momentum conservation reproduces well the Fokker-Planck results from the code CQL3D, while the high-speed-limit can significantly underestimate the current drive. One of the solvers that has been developed (based on the numerical fit and weakly-relativistic expansion) is being routinely for ECCD calculations for both tokamaks and stellarators.

It is important to mention also that while the current drive for tokamaks can be calculated with both the adjoint technique and the bounce-averaged Fokker-Planck code, for stellarators only the adjoint technique can be applied. Indeed, the drift-kinetic equation for stellarators (contrary to tokamaks) cannot be rigorously reduced to 3 variables (or, if to omit the radial diffusion, to 2 varuables in momentum space). Practically, it can be done only for some partial cases [11, 43]. Since the numerical solvers [27, 30] developed recently are already sufficiently rapid and accurate, the adjoint technique used in ray- and beam-tracing codes covers practically the whole spectrum of tasks for ECCD calculations.

In the paper, only the case of "low" collisionality was considered. While for hot plasmas in the ITER-scale tokamaks this approach is well applicable, for high-density and moderate temperature plasmas in stellarators like W7-X (especially in reactor-sized stellarators with large aspect ratio), the finite collisionality effects can produce a non-negligible contribution. Furthermore, these effects can also be important in tokamaks of the present generation. These effects are most complicated for consideration and to date no generally accepted model has been developed. From our point of view, the main emphasys of future work must be directed to these effects. Since some progress in this direction has already bin obtained [30, 39, 44–46], the preliminary results will be published in a coming paper.

Acknowledgments

The authors would like to acknowledge Yuriy Turkin for help and Per Helander for support and the additional references to this problem.

This work, supported by the European Community under the contract of Associations between EURATOM, IPP Greifswald, and the Austrian Academy of Sciences, was carried out within the framework of the European Fusion Development Agreement. The views and opinions expressed herein do not necessarily reflect those of the European Commission.

APPENDIX A: TOROIDAL CURRENT IN RAY-TRACING SIMULATIONS

Since the formulas necessary for numerical calculations of the toroidal current drive in ray- and beam-tracing codes are rather dispersed in the literature, it seems meaningful to collect the main definitions here. All definitions given below are valid for an arbitrary 3D magnetic configuration and do not depend on the choice of the coordinate set.

The elementary toroidal current drive which circulates through the area δA between the neighboring flux-surfaces ψ and $\psi + \delta\psi$ (here, ψ is the flux-surface label) can be defined in two alternative forms:

$$\delta I_{\rm tor} = \int_{\delta A} \left(\frac{j_\parallel}{B}\right) \mathbf{B}\cdot \mathrm{d}\mathbf{S} = \frac{\langle j_\parallel \rangle}{\langle B\rangle}\,\delta\Psi_{\rm tor} = \frac{\langle j_\parallel B\rangle}{\langle B^2\rangle}\,\delta\Psi_{\rm tor}, \tag{A1}$$

where $\Psi_{\rm tor}$ is the toroidal magnetic flux. Since the efficiency, η, and not $\langle j_\parallel \rangle$ directly, is calculated in the ray- and beam-tracing codes, there is the current drive generated on the elementary arc-length at the given ray in use,

$$\frac{dI_{\rm tor}}{ds} = \left(\langle B\rangle\, V'\right)^{-1}\,\eta\,\frac{dP_{\rm abs}}{ds}, \tag{A2}$$

where $V' = dV/d\Psi_{\rm tor}$, V is the volume within the magnetic surface ψ, $dP_{\rm abs}/ds = P_0\,\alpha\,\mathrm{e}^{-\tau}$ the power absorbed on the elementary arc-length, α is the cyclotron absorption coefficient, and $\tau = \int_0^s \alpha\, ds$ the optical depth. Then the elementary toroidal current for the given ray can be

calculated from

$$\frac{\delta I_{\rm tor}}{\delta \Psi_{\rm tor}} = V' \left| \frac{\delta V}{\delta s} \right|^{-1} \cdot \frac{dI_{\rm tor}}{ds}, \qquad \text{(A3)}$$

where $\delta V/\delta s$ is the rate of change of the volume along the ray trajectory. Summing the elementary contributions from all rays, the total toroidal current can be calculated by direct integration of Eq. (A3). When necessary, the value $\langle j_\parallel \rangle$ can also be obtained from Eq. (A1) and Eq. (A3).

Apart from $I_{\rm tor}$ and $\langle j_\parallel \rangle$, in the tokamak literature (see, e.g. [7, 28]) the density of the toroidal current, $j_{\rm tor}(\psi)$, is frequently used. Numerically, this value differs from $\langle j_\parallel \rangle$ only by a "geometrical factor", which depends on the magnetic configuration. Strictly speaking, $j_{\rm tor}(\psi)$ is not necessary for performing calculations, but may be useful for interpretation of the results. Apart from this, $j_{\rm tor}(\psi)$ can be defined in a unique way only for axisymmetric configurations, while for an arbitrary 3D configuration only the conventional definition can be introduced.

By definition, the toroidal current density is $j_{\rm tor} = \delta I_{\rm tor}/\delta A$, where $\delta I_{\rm tor}$ is expressed by Eq. (A1). In order to make it well defined, one needs to find the relation between the elementary magnetic flux $\delta\Psi_{\rm tor}$ and the elementary cross-section area, δA. In the general magnetic flux coordinates (ψ, θ, φ) with θ and φ the poloidal and toroidal angles, respectively, the elementary toroidal flux between the neighboring magnetic surfaces is given by

$$\delta\Psi_{\rm tor} = \int_{\delta A} (\mathbf{B}\cdot\nabla\varphi)\,\sqrt{g}\,d\theta\,d\psi = \frac{1}{2\pi}\,\delta V\,\langle \mathbf{B}\cdot\nabla\varphi\rangle\,, \qquad \text{(A4)}$$

where $\sqrt{g}$ is the Jacobian. While the toroidal flux is the function of only the flux-surface label, $\delta\Psi_{\rm tor} \equiv \delta\Psi_{\rm tor}(\psi)$, the elementary area in the toroidal cross-section $\varphi = Const$ in arbitrary 3D configuration is more complex, $\delta A \equiv \delta A(\psi, \varphi)$. On the other hand, one can introduce the conventional elementary area averaged around the torus,

$$\overline{\delta A} \doteq \frac{1}{2\pi}\int_0^{2\pi} d\varphi \int_{\delta A} |\nabla\varphi|\,\sqrt{g}\,d\theta\,d\psi = \frac{1}{2\pi}\,\delta V\,\langle|\nabla\varphi|\rangle\,, \qquad \text{(A5)}$$

which leads to the relation

$$\delta\Psi_{\rm tor} = \overline{\delta A}\,\frac{\langle \mathbf{B}\cdot\nabla\varphi\rangle}{\langle|\nabla\varphi|\rangle} \qquad \text{(A6)}$$

and to the final expression for the "conventional" toroidal current density:

$$j_{\rm tor}(\psi) \doteq \frac{\delta I_{\rm tor}}{\overline{\delta A}} = \langle j_\parallel\rangle\,\frac{\langle \mathbf{B}\cdot\nabla\varphi\rangle}{\langle B\rangle\,\langle|\nabla\varphi|\rangle}, \qquad \text{(A7)}$$

which is the product of an average parallel current density and a geometrical factor. The physical meaning of $j_{\rm tor}(\psi)$ is the average toroidal current density at the magnetic surface.

For the axisymmetric (tokamak) configurations, Eq. (A7) is uniquely defined due to an equivalence $\overline{\delta A} = \delta A$. In the flux-coordinates $(\Psi_{\rm pol}, \theta, \phi)$, where $\Psi_{\rm pol}$ is the poloidal flux and ϕ is the toroidal symmetry angle (the surfaces $\phi = Const$ are the vertical planes with $|\nabla\phi| = 1/R$), the magnetic field in tokamaks can be represented as

$$\mathbf{B} = F(\psi)\nabla\phi + \frac{1}{2\pi}\nabla\phi\times\nabla\Psi_{\rm pol}, \qquad \text{(A8)}$$

where $F(\psi)$ is the poloidal current function. Then the toroidal current density can be easily obtained,

$$j_{\rm tor}(\psi) = \langle j_\parallel\rangle\,\frac{F(\psi)\,\langle 1/R^2\rangle}{\langle B\rangle\,\langle 1/R\rangle}, \qquad \text{(A9)}$$

where the tokamak's "geometrical factor" coincides with that obtained in [7].

[1] T. Ohkawa, *Steady-state operation of tokamaks by rf heating* (1976), General Atomics Report GA-A13847.

[2] N. J. Fisch and A. H. Boozer, Phys. Rev. Lett. **45**, 720 (1980).

[3] N. J. Fisch, Rev. Mod. Physics **59**, 175 (1987).

[4] C. F. F. Karney and N. J. Fisch, Phys. Fluids **28**, 116 (1985).

[5] R. H. Cohen, Phys. Fluids **30**, 2442 (1987), and **3**1, 421 (1988).

[6] M. Taguchi, Plasma Phys. Control. Fusion **31**, 241 (1989).

[7] Y. R. Lin-Liu, V. S. Chan, and R. Prater, Phys. Plasmas **10**, 4064 (2003).

[8] R. Prater, Phys. Plasmas **11**, 2349 (2004).

[9] K. Nagasaki, A. Isayama, N. Hayashi, T. Ozeki, M. Takechi, N. Oyama, S. Ide, S. Yamamoto, and the JT-60 Team, Nuclear Fusion **45**, 1608 (2005).

[10] H. Zohm, G. Gantenbein, F. Leuterer, A. Manini, M. Maraschek, Q. Yu, and the ASDEX Upgrade Team, Nuclear Fusion **47**, 228 (2007).

[11] H. Maaßberg, M. Rome, V. Erckmann, J. Geiger, H. P. Laqua, N. B. Marushchenko, and the W7-AS Team, Plasma Phys. Control. Fusion **47**, 1137 (2005).

[12] R. W. Harvey and M. G. McCoy, in *Proc. IAEA Tech. Comm. Meeting 1992* (IAEA, Vienna, 1993), p. 498.

[13] C. C. Petty, R. Prater, T. C Luce, R. A. Ellis, R. W. Harvey, J. E. Kinsey, L. L. Lao, J. Lohr, M. A. Makowski, and K.-L. Wong, Nuclear Fusion **43**, 700 (2003).

[14] T. C. Luce, Y. R. Lin-Liu, R. W. Harvey, G. Giruzzi, J. M. Lohr, C. C. Petty, P. A. Politzer, R. Prater, and R. W. Rice, Plasma Phys. Control. Fusion **41**, B119 (1999).

[15] S. P. Hirshman, Phys. Fluids **23**, 1238 (1980).

[16] T. M. Antonsen and K. R. Chu, Phys. Fluids **25**, 1295 (1982).

[17] L. Spitzer and R. Härm, Phys. Rev. **89**, 977 (1953).

[18] F. L. Hinton and R. D. Hazeltine, Rev. Mod. Physics **48**, 239 (1976).

[19] N. J. Fisch, Phys. Fluids **29**, 172 (1986).

[20] C. F. F. Karney and N. J. Fisch, Phys. Fluids **29**, 180 (1986).

[21] B. J. Braams and C. F. F. Karney, Phys. Fluids B **1**, 1355 (1989).

[22] M. Taguchi, J. Phys. Soc. Jpn. **51**, 1975 (1982).

[23] M. Taguchi, J. Phys. Soc. Jpn. **52**, 2035 (1983).

[24] T. M. Antonsen and B. Hui, IEEE Trans. Plasma Sci. **PS-12**, 118 (1984).

[25] C. F. F.Karney, N. J. Fisch, and A. H. Reiman, in *AIP Conf. Proc.* (1989), 190, p. 430.

[26] S. C. Chiu, C. F. F.Karney, T. K. Mau, and Y. R. Lin-Liu, Phys. Plasmas **2**, 450 (1995).

[27] S. V. Kasilov and W. Kernbichler, Phys. Plasmas **3**, 4115 (1996).

[28] R. Prater, D. Farina, Yu. Gribov, R. W. Harvey, A. K. Ram, Y. R. Lin-Liu, E. Poli, A. P. Smirnov, F. Volpe, E. Westerhof, et al., Nuclear Fusion **48**, 035006 (2008).

[29] N. B. Marushchenko, H. Maassberg, and Yu. Turkin, Nuclear Fusion **48**, 054002 (2008), and **49** 129801 (2009).

[30] N. B. Marushchenko, C. D. Beidler, and H. Maassberg, Fusion Sci. Technol. **55**, 180 (2009).

[31] N. B. Marushchenko, V. Erckmann, H.-J. Hartfuss, M. Hirsch, H. P. Laqua, H. Maassberg, and Yu. Turkin, Jpn. J. Plasma Fusion Res. **2**, S1000 (2007), (http://www.jspf.or.jp/PFR/PDF/pfr2007_02-S1129.pdf).

[32] J. G. Cordey, Nuclear Fusion **16**, 499 (1976).

[33] M. Romé, V. Erckmann, U. Gasparino, and N. Karulin, Plasma Phys. Control. Fusion **40**, 511 (1998).

[34] N. B. Marushchenko, V. Erckmann, H. P. Laqua, H. Maaßberg, and Yu. Turkin, in *Proc. 34th EPS Conference on Plasma Phys. Warsaw, 2 - 6 July 2007 ECA Vol.31F, P-5.129 (2007)* (2007).

[35] N. B. Marushchenko, H. Maassberg, C. D. Beidler, V. Erckmann, J. Geiger, A. G. Shalashov, E. V. Suvorov, Yu. Turkin, and W7-X Team, in *Proc. VII Int. Workshop "Strong Microwaves: Sources and Applications", Nizhny Novgorod, 27 July - 2 August 2008* (IAP RAS, Nizhny Novgorod, 2009), vol. 1, p. 375.

[36] F. Wagner, A. Becoulet, R. Budny, V. Erckmann, D. Farina, G. Giruzzi, Y. Kamada, A. Kaye, F. Koechl, K. Lackner, et al., Plasma Phys. Control. Fusion **52** (2010).

[37] K. Nagasaki, S. Yamamoto, H. Yoshino, K. Sakamoto, N. B. Marushchenko, Y. Turkin, T. Mizuuchi, H. Okada, K. Hanatani, T. Minami, et al., in *Proc. 23rd IAEA Fusion Energy Conference, Daejeon, Rep. of Korea, 11 - 16 October, 2010, IAEA-CN-180/EXW/P7-19* (2010).

[38] J. M. García-Regaña, F. Castejon, A. Cappa, N. B. Marushchenko, and M. Tereshchenko, Plasma Phys. Control. Fusion **52**, 065007 (2010).

[39] H. Maaßberg, C. D. Beidler, and Y. Turkin, Phys. Plasmas **16**, 072504 (2009).

[40] K. Matsuda, IEEE Trans. Plasma Sci. **17**, 6 (1989).

[41] A. P. Smirnov, R. W. Harvey, and K. Kupfer, Bull. Am. Phys. Soc. **39**, 1626 (1994).

[42] A. P. Smirnov and R. W. Harvey, in *Proc. 15th Joint Workshop on ECE and ECRH, Yosemity Park, California, 10-13 March 2008* (World Scientific Publishing Co. Pte. Ltd., 5 Toh Tuck Link, Singapure 596224, 2009), p. 301.

[43] N. Marushchenko, U. Gasparino, H. Maaßberg, and M. Romé, Comp. Phys. Comm. **103**, 145 (1997).

[44] Y. R. Lin-Liu, O. Sauter, R. W. Harvey, V. S. Chan, T. C. Luce, and R. Prater, in *Proc. 26th EPS Conf. on Contr. Fusion and Plasma Physics, Maastricht, 14 - 18 June 1999 ECA Vol.***23J** *(1999) 1245 - 1248, P3.078* (1999), vol. 23J, pp. 1245 – 1248.

[45] M. Romé, C. D. Beidler, S. V. Kasilov, W. Kernbichler, G. O. Leitold, H. Maaßberg, N. B. Marushchenko, V. V. Nemov, and Yu. Turkin, in *Proc. 36th EPS Conf. on Plasma Phys., Sofia, June 29 - July 3, 2009 ECA Vol.***33E** *(2009), P-1.136* (2009), vol. 33E, pp. 1245 – 1248.

[46] W. Kernbichler, S. V. Kasilov, G. O. Leitold, V. V. Nemov, and N. B. Marushchenko, Contrib. Plasma Phys. **50**, 761 (2010).